Journal of Petroleum Research and Studies

journal homepage: https://jprs.gov.iq/index.php/jprs/

Print ISSN 2220-5381, Online ISSN 2710-1096

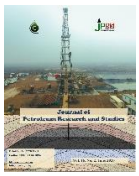

Impact of Dual-Fuel Diesel/Hydrogen on The Performance and Emissions of Internal Combustion Engine

Ahmed E. Hamdi*, Rafid M. Hannun

Mechanical Engineering Department, Faculty of Engineering, University of Thi-Qar, Thi-Qar, Iraq.

*Corresponding Author E-mail: ahmeden2005@utq.edu.iq

Article Info

Received 11/12/2024
Revised 13/02/2025
Accepted 25/02/2025
Published 21/06/2026

DOI: http://doi.org/10.52716/jprs.v16i2.1054

Abstract

This study investigates the effects of hydrogen-assisted combustion of n-heptane on engine performance, combustion behavior, and emission characteristics. The simulation was performed on a diesel engine fueled by n-heptane with 10% and 20% hydrogen injection volumes. The combustion simulation was performed on a three-dimensional cylindrical sector, with the engine speed maintained at 2000 revolutions per minute (rpm) while the crank angle varied from 570° to 833°. A reaction mechanism was utilized to incorporate the phases of n-heptane and H_2 interaction and the CO and NOx formation processes. According to the modeling results, increasing hydrogen induction dramatically improves performance by raising the maximum cylinder pressure, brake thermal efficiency, and heat release rate. The cylinder pressure increases by 4.1% and 15.9% when 10% and 20% hydrogen are added to heptane, respectively. Adding 10% H_2 increases the thermal efficiency by 23.7%, and adding 20% H_2 increases it by 37%. Together with the contours of CO, CO_2, and NOx, the distribution of in-cylinder pressure illustrates the properties of the flow field. Both CO and CO_2 pollution have significantly decreased overall. When a 10% volume of H_2 was added, CO emissions dropped by 57.1%, and when a 20% volume of H_2 was added, they dropped by 64.2%. CO_2 emissions decreased by 25.1% with a 10% volume of H_2 and by 39.1% with a 20% volume of H_2. Moreover, more excellent combustion has resulted in a rise in NOx emissions.

Keywords: IC Engine, H_2, Dual fuel, N-heptane, modeling.

دراسة تأثير استخدام وقود الديزل الهيدروجيني المزدوج على أداء المحرك والانبعاثات

الخلاصة:

تبحث هذه الدراسة في تأثيرات احتراق الن-هيبتان بمساعدة الهيدروجين على أداء المحرك وسلوك الاحتراق وخصائص الانبعاث. تم إجراء المحاكاة على محرك ديزل يعمل بالهيبتان الطبيعي بحجم حقن هيدروجين 10٪ و 20٪. تم إجراء محاكاة الاحتراق على قطاع أسطواني ثلاثي الأبعاد، مع الحفاظ على سرعة المحرك عند 2000 دورة في الدقيقة (rpm) بينما تراوحت زاوية العمود المرفقي من 570 درجة إلى 833 درجة. تم استخدام آلية تفاعل لدمج مراحل تفاعل الن-هيبتان والهيدروجين وعمليات تكوين أول أكسيد الكربون وأكاسيد النيتروجين. وفقًا لنتائج النمذجة، فإن زيادة تحريض الهيدروجين يحسن الأداء بشكل كبير من خلال رفع الحد الأقصى لضغط الأسطوانة وكفاءة الحرارة للفرامل ومعدل إطلاق الحرارة. يزداد ضغط الأسطوانة بنسبة 4.1٪ و 15.9٪ عند إضافة 10٪ و 20٪ من الهيدروجين إلى الهبتان على

التوالي. إن إضافة 10% من الهيدروجين تزيد من الكفاءة الحرارية بنسبة 23.7%، وإضافة 20% من الهيدروجين تزيدها بنسبة 37%. جنبًا إلى جنب مع خطوط أول أكسيد الكربون وثاني أكسيد الكربون وأكاسيد النيتروجين، يوضح توزيع الضغط داخل الأسطوانة خصائص مجال التدفق. انخفض تلوث أول أكسيد الكربون وثاني أكسيد الكربون بشكل كبير بشكل عام. عند إضافة 10% من حجم الهيدروجين، انخفضت انبعاثات أول أكسيد الكربون بنسبة 57.1%، وعند إضافة 20% من حجم الهيدروجين، انخفضت بنسبة 64.2%. انخفضت انبعاثات ثاني أكسيد الكربون بنسبة 25.1% مع 10% من حجم الهيدروجين وبنسبة 39.1% مع 20% من حجم الهيدروجين. علاوة على ذلك، أدى الاحتراق الأفضل إلى زيادة انبعاثات أكاسيد النيتروجين.

1. Introduction

The oil industry occupies an important place in the world economy. Oil and petroleum products meet energy needs in several industries, such as small-scale consumption, factories, and transportation. The consequences of global climate change and the growing number of cars have made using fossil fuels a hot topic. In the world, oil products are the primary energy source, especially internal combustion engines utilized for energy production and transportation [1].

The current explosion in research and technological developments about hydrogen has mainly affected Europe, as it is motivated by the strong desire to reach the goal of net zero greenhouse gas (GHG) emissions by 2050. The transportation sector causes twenty-five percent of greenhouse gas emissions in the EU. The European Green Deal mandates a 90% reduction in emissions by 2050 [2]. To address the emissions problem linked to road transport, pivotal stakeholders in the energy transition, including government entities and private automotive companies, are increasingly transitioning from conventional technologies such as internal combustion engines (ICEs) to electric vehicles and alternative fuels. Hydrogen-fueled internal combustion engines (H_2-ICEs) and fuel cell electric vehicles (FCEVs) are effective alternatives for alleviating the environmental impacts linked to conventional autos. Additionally, by improving current internal combustion engines (ICEs) without needing batteries or fuel cells, H_2-ICEs can more economically support the transition to low-carbon transportation. Although burning H_2 produces no CO_2 emissions, it does produce nitrogen oxides (NOx) emissions [3].

The absence of carbon atoms in the H_2 molecule makes for eco-friendly combustion with minimal emissions of greenhouse gases. Furthermore, when comparing H_2 with traditional fuels, the lower heating value (LHV), which calculates the energy released per unit mass during fuel combustion, is almost three times higher for H_2. This illustrates the considerable potential of H_2 as a clean energy conduit. However, owing to its lower molecular weight, it demonstrates the least density, leading to diminished power density in the gaseous phase, quantified per unit volume. The elevated laminar flame speed (SL) of H_2 significantly boosts combustion efficiency by augmenting chemical reactivity [4].

1.1. Literature review

Numerous studies have used hydrogen as a substitute fuel for many different diesel engines, and their results show how hydrogen affects engine performance and combustion. Estrada et al. [5] showed that using hydrogen decreased brake-specific fuel consumption, increased thermal efficiency, reduced CO and HC emissions, diminished CO_2 emissions, and heightened NOx emissions. Kavtaradze et al. [6] elucidated the principal advantages of hydrogen consumption, including enhanced fuel efficiency, diminished pollutant emissions (notably soot and nitrogen oxides), and lowered greenhouse gas emissions (particularly CO_2). Nevertheless, the maximum pressure could rise as a result of hydrogen combustion. Koten et al. [7] employed hydrogen as a diesel engine fuel in their research. They discovered that for all hydrogen flows, decreasing soot emissions and increasing brake-specific fuel consumption were the outcomes of adding hydrogen to the engine intake.

Nonetheless, they also noted a rise in NOx emission levels, especially under elevated engine loads. Zhang et al. [8] reported incorporating a hydrogen fraction (15% to 35%) enhanced engine thermal efficiency.

Nevertheless, the concentration of NOx emissions rose to 83% relative to the air-fuel ratio. An increase in hydrogen concentration resulted in an estimated 30% rise in maximum pressure and a 66% increase in the peak rate of pressure expansion during combustion. Demirci et al. [9] discovered that injecting moderate quantities of hydrogen into the engine inlet decreases brake-specific fuel and energy consumption alongside enhanced engine thermal efficiency. NOx emissions also rise when the hydrogen dose is increased at full load. Up to a maximum of 2.5%, NOx emissions decreased at various working loads as hydrogen rose. The soot emission level decreased by 27.5% when the maximum quantity of hydrogen was utilized. Under full load conditions, CO_2 emissions diminish by 0.81%. Under other operating circumstances, however, the reduction in CO_2 emissions is more significant and can reach 12.6%, contingent on the quantity of hydrogen utilized.

According to the research by Sughayyer et al. [10], using hydrogen increased engine power and decreased emissions of pollutants, especially carbon monoxide (CO). In their explanation, Loganathan et al. [11] stated that using hydrogen increases combustion pressure. The maximum combustion pressure can be reduced by applying Exhaust Gas Recirculation (EGR).

Moreover, using EGR causes a rise in the cyclic variations of peak pressure measurements. Ghazal [12] developed a computer model mimicking a diesel engine's hydrogen utilization. This simulation resulted in a decrease in pollutant emissions and a decline in the rate of pressure

increase. Deb et al. [13] experimented with changing the amount of hydrogen in the fuel mixture for a diesel engine running at 1500 rpm with little load. They found that employing hydrogen reduced brake-specific energy consumption (BSEC) and increased brake thermal efficiency. CO_2 and soot emissions fall as the hydrogen content rises, whereas NOx emissions rise as the hydrogen content rises. Karagoz et al. [14] noted that the incorporation of hydrogen in a diesel engine results in heightened brake-specific fuel consumption and diminished thermal efficiency at all operational speeds. Incorporating 25% hydrogen led to a 25% reduction in CO_2 emissions and a 51% reduction in smoke emissions. Incorporating 25% hydrogen resulted in a peak increase of 39% in NOx emissions. After adding 50% hydrogen, smoke emissions are reduced by 58%, CO_2 levels diminish by 38%, and NOx levels rise by almost 200%. The maximum pressure rose by 11% with a hydrogen concentration of 25% and 34% with a hydrogen concentration of 50%. Morais et al. [15] did a study that revealed a 12% reduction in CO_2 emissions when 20% hydrogen is utilized as a substitute for diesel fuel in a diesel engine. This decrease in emissions is accomplished while preserving a comparable level of engine efficiency relative to conventional diesel fuel. In an experiment by Kose et al. [16], they powered a turbo-supercharged diesel engine with different percentages of hydrogen, ranging from 2.5% to 7.5%. The results indicated increased hydrogen concentration corresponded with increased thermal efficiency and NOx emissions levels. Fuel consumption diminished with minimal hydrogen quantities, specifically 2.5% and 5%, but experienced a tiny increase when the hydrogen proportion escalated to 7.5%. The utilization of hydrogen generally diminishes CO_2 emissions, with the reduction being more pronounced as the quantity of hydrogen escalates. According to the research by Adnan et al. [17], the addition of hydrogen guaranteed an increase in the peak pressure during combustion, ranging from 5 bar to more than 20 bar, depending on the cyclic concentration of hydrogen. NOx and CO_2 emissions rose by 50-200 ppm and 1%-4%, respectively, for the equivalent percentage of hydrogen.

1.2. Aims and Objectives

This study aims to investigate the efficiency, combustion properties, and emissions of n-heptane combustion in detail. It also seeks to reduce the discrepancy in using hydrogen as an alternative to fossil fuels and analyze the effects of adding hydrogen to the engine. A comprehensive reaction mechanism is constructed to study the kinetics of the reaction between n-heptane and hydrogen while accounting for the mechanisms that result in the creation of CO_2 and NOx.

2. Methodology

2.1. Governing Equations

Fundamental ideas can characterize turbulent flows and enable their representation as governing differential equations. One method for solving or modeling these equations is computational fluid dynamics (CFD).

2.1.1. Continuity Equation

The conservation of mass, sometimes known as the continuity equation, for a compressible fluid can be expressed theoretically as equation (1) [18]:

$$\frac{\partial}{\partial t}(\rho) + \frac{\partial}{\partial x_i}(\rho u_i) = S_m, \quad (1)$$

Where (ρ) represents the fluid's density, and (t) signifies time. (u_i) represents the component of the velocity vector. (x_i) represents the component of the position vector. (S_m) represents mass contributed to the continuous phase by the dispersed phase.

2.1.2. Momentum Equation

From Newton's second law, the idea of conservation of momentum is inferred, as show in equation (2).

$$\frac{\partial}{\partial t}(\rho u_j) + \frac{\partial}{\partial x_i}(\rho u_i u_j) = -\frac{\partial}{\partial x_j}(P) + \frac{\partial}{\partial x_i}(\tau_{ij}) + \rho g_i + S_i, \quad (2)$$

Where (t, P,τ_{ij} and ρg_i) represent time, pressure, viscous stress, and gravitational body force, respectively. (S_i) represents the exterior body forces.

The equation representing momentum per unit volume in the y and z-directions can also be articulated.

2.1.3. Energy Equation

The first law of thermodynamics quantitatively articulates the principle of energy conservation as equation (3).

$$\frac{\partial}{\partial t}(\rho h) + \frac{\partial}{\partial x_i}(\rho u_i h) = \frac{\partial}{\partial x_i}\left(\frac{\lambda}{c_p}\frac{\partial h}{\partial x_i}\right) + \frac{\partial}{\partial x_i} Dh + \mathcal{S}h, \quad (3)$$

Where (h) the total enthalpy. (λ) represent the effective conductivity. (c_p) represents the specific heat capacity of the fluid. $(\mathcal{S}h)$ represents the source term that accounts for any supplementary heat losses.

2.2. Assumptions of Flow

To solve the governing equations, the following assumptions were taken into account:

1- Un steady-state flow.

2- Turbulent flow.
3- Three-dimensional flow.
4- Incompressible flow.

2.3. Turbulence Modelling

The fluid flow can be categorized into two distinct classifications: laminar and turbulent. Turbulence presents a significant challenge when attempting to model any real-world flow. Turbulence is a common occurrence in many real-world flows and refers to the unpredictable and chaotic variation of flow parameters. This poses numerous challenges in modelling, as accounting for every minute variance would result in exorbitant computational costs, rendering direct calculation impractical in most scenarios.

Turbulence can be defined by the Reynolds number, which is defined as the ratio of inertial forces to viscous forces. The Reynolds number represents the threshold at which the flow exhibits distinct behavior. Below the critical point, the flow exhibits a smooth, consistent, and regular pattern known as laminar flow. However, above this point, the flow undergoes considerable fluctuations, resulting in an unsteady, unpredictable, and disorderly flow known as turbulent flow.[19]

2.3.1. Standard K-epsilon Model

The model (standard k-ε) is adopted to represent the turbulence in this modeling. The standard k-ε model is a turbulence model that utilizes two additional transport equations: one for the turbulent kinetic energy, k, and another for the dissipation rate of turbulent kinetic energy, ε. The transport equation for k is derived from the precise equation, whereas the transport equation for ε is found by physical reasoning and has minimal similarity to its mathematically exact equivalent.

2.4. Geometric Design

With ANSYS Workbench 16.0, the combustion computational fluid dynamics (CFD) simulation was carried out utilizing the software's built-in IC Engine code. The finite volume method is employed to resolve the governing equations of fluid dynamics. An engine that was constructed using AutoCAD and then put into ANSYS WORKBENCH for proper modeling was used in the simulation. Four valves are contained in the engine's single cylinder, two of which are intake valves, and the other two are exhaust valves, as seen in Figure (1). The engine

is characterized by a 90 mm bore and a 110 mm stroke. It includes a connecting rod measuring 165 mm in length. Table (1) presents the engine specifications, which indicate a 15.83 compression ratio. A sector of the cylinder can be employed at a 60-degree angle thanks to the fuel injector's combustion chamber's six identical holes, as seen in Figure (2). The judicious use of sectors markedly decreases computation costs.

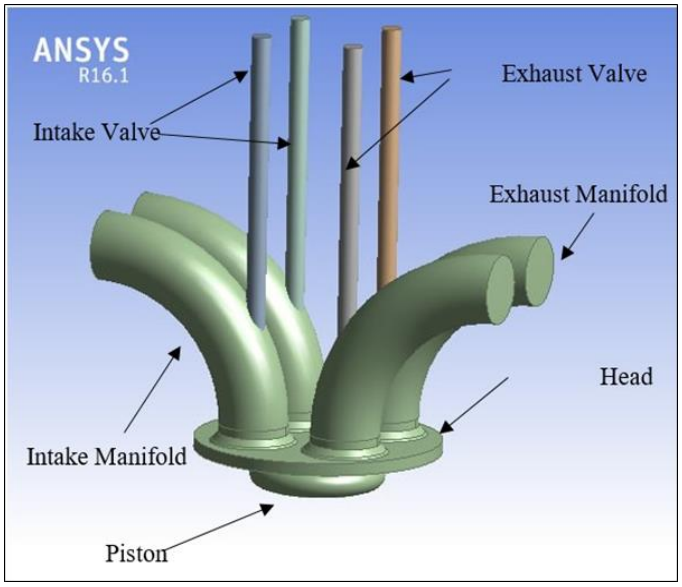

Fig. (1): Geometry of the engine

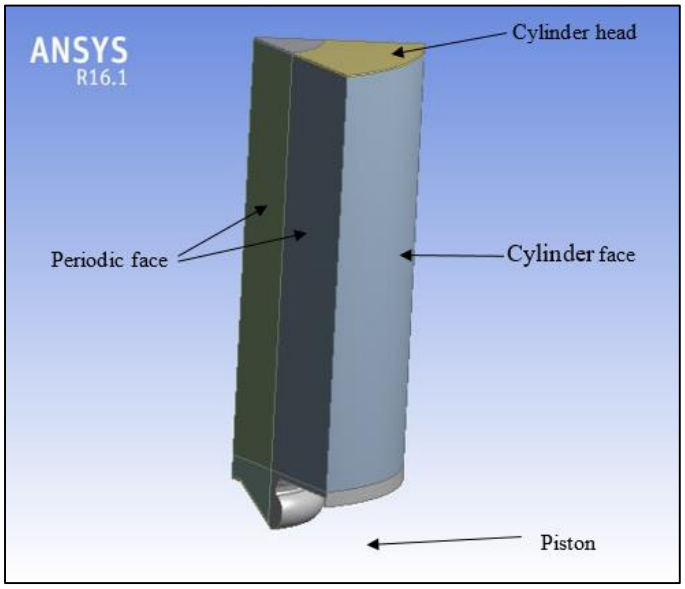

Fig. (2): Sector of the cylinder

Crankshaft rotation occurs during engine operation, and it is connected to the piston, which moves vertically via a connecting rod. A volume inside the cylinder corresponds to each crank angle degree. The simulation within the framework encompasses a range of crank angles (CA)

from 570° to 833°, with the top dead center (TDC) established at 720°. The simulation is carried out in a sector that spans the time interval between the intake valve closing (IVC) and the exhaust valve opening (EVO), during which all valves stay tightly closed. Consequently, both the intake and exhaust ports, as well as their respective valves, are excluded.

Table (1): The specifications of the engine

Parameter	Value
Bore	90 mm
Stroke	110 mm
Crank radius	55 mm
Connecting rod	165 mm
Compression ratio	15.83
Engine speed	2000 rpm
Intake valve closed (IVC)	570° CA
Exhaust valve open (EVO)	833° CA

2.5. Meshing

Next came the creation of the 3D model's mesh or grid. Often called a grid or mesh of cells, the mesh aims to separate the field into several smaller, discrete subdomains where the model is set for solution. This step is crucial since the solution's accuracy, convergence, and speed in (CFD) simulation strongly correlate with the mesh quality. In this case, the meshing approach was prioritized, as the engine components, including the piston and valves, were equipped with a dynamic mesh[20]; this technique facilitates the simulation of issues associated with changing boundary motion. This method results in a variable control volume, which undergoes continuous movement and alteration. The mesh will undergo validation subsequently. Figure (3) illustrates the sector's mesh. The organized mesh is present across a significant portion of the computational domain. In proximity to the piston, supplementary cells and hexahedrons facilitate the precise positioning of the piston crown.

Fig. (3): Mesh of the sector

2.5.1. Mesh Validation

Two meshes covering a 60° sector each—coarse and fine mesh- were created for the engine's basin form to accomplish mesh autonomy. There are 610796 nodes and 584812 components in the coarse mesh. In contrast, the fine mesh has 1035512 nodes and 998408 components. Table (2) shows the specifications for each mesh. Notwithstanding the coarse mesh's comparatively large size compared to standard computational fluid dynamics (CFD) applications, the polar sector mesh has an adequate number of tiny cells close to the injector spout and fuel jet path to depict the injection process accurately. Under the specified circumstances, each mesh's cylinder pressure forms were tested using diesel fuel at 1500 rpm.

Table (2): The specifications of coarse and fine mesh

Parameter	Coarse mesh	Fine mesh
Nodes	610796	1035512
Elements	584812	998408
Minimum Size	0.190 mm	0.127 mm
Maximum Size	0.474 mm	0.316 mm

Upon thorough study, it is evident that additional improvements to the mesh did not produce any noticeable alterations in the expected cylinder pressure, as illustrated in Figure (4). Consequently, a coarse mesh was utilized for all simulations to reduce processing time.

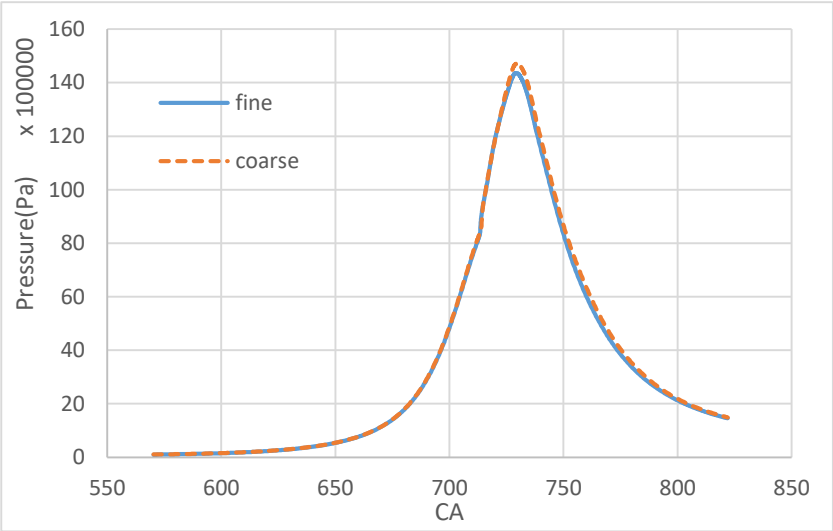

Fig. (4): In-cylinder pressure for n-heptane, at fine and coarse mesh."

2.6. IC Engine Solver Settings

This section provides a comprehensive account of the parameters and operational conditions utilized to execute the modeling process effectively. The swirl number was set to 1.3, and the engine was calibrated to run at 2000 rpm. The simulation range was set between 570° and 833° with a timestep size of 0.25 step/CA, except for the fuel injection phase, which was limited to 0.05 step/CA for each crank. There were 50 iterations needed for each time step.

As indicated in Table (3), the beginning conditions were set at a temperature of 313 Kelvin, a pressure of 1 bar, and velocities of 0 meters per second in the x, y, and z directions. The symmetry of the injectors is used to divide the domain into sectors, and the side surfaces of each sector are subject to periodic boundary conditions. Constant temperature boundary conditions govern heat transfer at the interfaces between gas and solid, presuming that the engine has undergone several cycles prior. The piston's surface temperature is 600 K, the cylinder wall temperature is 400 K, and the surface temperature of the cylinder is 450 K. Table (3) delineates the designated initial and boundary conditions.

Table (3): Initial and Boundary conditions"

Initial conditions	value	Boundary conditions	value
Pressure	101325 (Pa)	Piston	600 (K)
Temperature	313 (K)	Head	450 (K)
x, y, and z velocities	0 (m/s)	Cyl chamber top	400 (K)
turbulent kinetic energy	1 (m^2/s^2)	Cyl chamber bottom	400 (K)
turbulent dissipation rate	1 (m^2/s^3)	Cyl piston	400 (K)

Diesel (n-heptane/C_7H_{16}) has been chosen as the fuel for the modeling technique. Another option is to mix hydrogen and fuel in the engine, which is fed into the software using a (chemkin file) which contains all the chemical reactions of the fuel components, with air as an oxidizer. The chemical reaction mechanism must be considered to comprehend the n-heptane combustion process. Consequently, the most comprehensive procedure was brought in. Additionally, the mechanism includes carbon monoxide (CO) and nitrogen oxide (NOx) computations. This mechanism comprises 325 reactions and 53 species [21], [22].

A 6-hole injector evenly distributed throughout the cylinder's volume is part of the engine. The diameter of each aperture is 0.13 mm. A precise location (x = 0.366, y = -0.41, and z = 0.366 mm) is used to discharge the spray, which is then directed inside the chamber at a 70° angle concerning the cylinder's axis. At a crank angle of 712° (CA), the injection procedure begins, and it ends at 310 K after 26° CA. The injection possesses a velocity of 525 m/s and a total flow rate of 0.0074 kg/s. The injector's specs are detailed in Table (4).

Table (4): The specifications of the injector

Parameter	Value
Fuel	n-heptane ($C_7 H_{16}$) and Hydrogen (H_2)
Nozzle diameter	0.13 mm
Injection start	712° CA
Injection end	738° CA
Spray direction	70°
Spray point coordinate	x= 0.366, y= -0.41, z= 0.366,
Velocity of injection	525 m/s
Mass flow rate of injection	0.0077 kg/s
Injection temperature	310 K
LHV of n-heptane	44.924 (MJ/kg)
LHV of hydrogen	120 (MJ/kg)

3. Results and Discussions

The objective is to examine the engine's combustion and mechanical properties. Analyzing the mean variations in cylinder pressure allows one to determine the engine's mechanical efficiency. On the other hand, combustion's effectiveness is assessed by examining changes in the average temperature within the cylinder along with variables like thermal efficiency, heat release rate, and NOx, CO, and CO2 production. In-cylinder combustion is modeled starting at 570° CA, or 150° CA before the top dead center (TDC), and ending at 833° CA, or 113° CA after TDC. The gasoline is injected at 712° CA, which is precisely 8 degrees CA ahead of the top dead center (TDC) and continues for 26 degrees CA.

3.1. Validation

We use a simulation model previously developed by Zahid et al. [3] in a literature analysis to verify the validity of the model in question. We examined the same working circumstances they used. The engine was running at 2000 rpm. A three-dimensional (3D) sector of the piston-cylinder assembly with a sector angle of 60 degrees serves as the engine's geometric model. During the simulation, the crank angle (CA) varies from 570 to 833 degrees. Figure (5) presents an assessment and presentation of the results derived from the current study and prior research. The diagram depicts the pressure within the cylinder for both analyses, demonstrating a significant degree of resemblance. The discrepancy in the results may attain up to 3.5%.

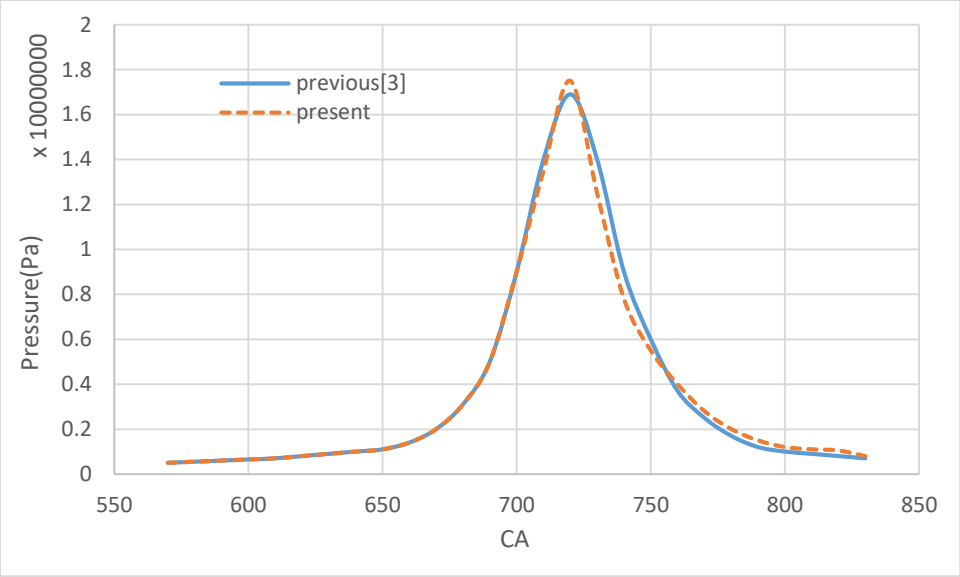

Fig. (5): In- cylinder pressure for present and previous studies

3.2. Pressure

The correlation between crank angle and volume-averaged static pressure is seen in Figure (6). Starting at 1 bar at 570° CA and rising to 115.1 bar at TDC, the in-cylinder pressure gradually increases due to the piston's upward motion during the compression stroke. When the cylinder is ignited, its pressure quickly rises to its highest point. This is determined by how well the hydrogen-oxygen mixture, which is well mixed in the cylinder, burns. Upon igniting, it combusts rapidly. As the combination finishes burning, the pressure inside the cylinder decreases, and the cylinder's volume increases. The cylinder's maximum pressure increased when 10% and 20% hydrogen were mixed with fuel. This is due to the elevated flame velocity and high thermal value of hydrogen. Figure 5 shows the pressure data recorded when hydrogen (H_2) was added. The maximum cylindrical pressure demonstrates a 4.1% increase when the

hydrogen level is 10% relative to the absence of hydrogen. It similarly demonstrates a 15.9% rise in H_2 energy amounts of 20%.

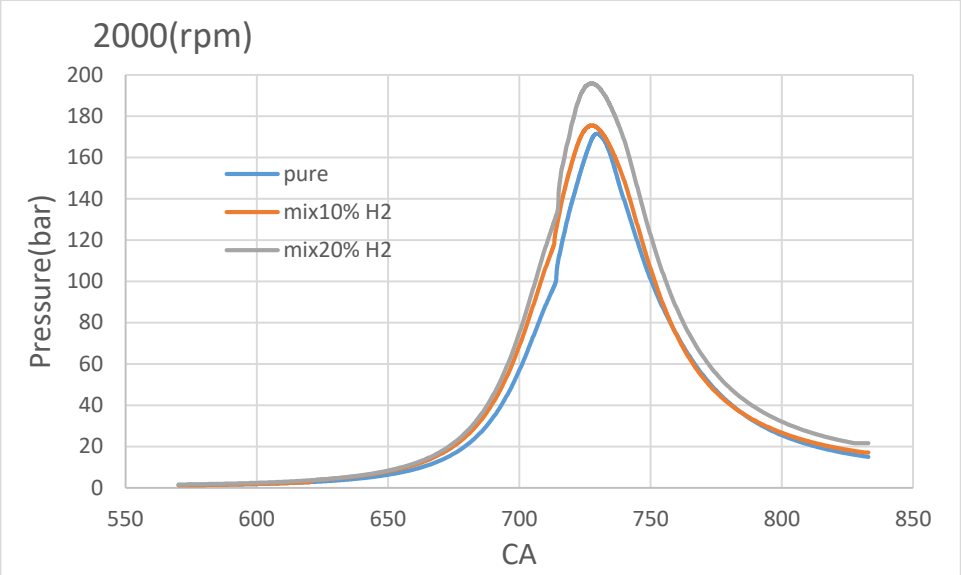

Fig. (6): In-cylinder pressure for pure fuel, 10% and 20% mixing of H_2

3.3. Break Thermal Efficiency (BTE)

The variation in break thermal efficiency (BTE) depending on the hydrogen energy content is shown in Figure (7). As the amount of hydrogen increases, the break thermal efficiency also increases. A 23.7% improvement in break thermal efficiency was obtained with 10% hydrogen injection, while a 37% increase was obtained with 20% hydrogen. Diesel fuel does not have the same flame speed as hydrogen fuel. Consequently, using hydrogen in diesel combustion will result in faster and more complete burning. As a result of this component, the in-cylinder pressure is elevated at its maximum, which also occurs at the top dead center [23]. As a result, there is an increase in the engine's thermal efficiency.

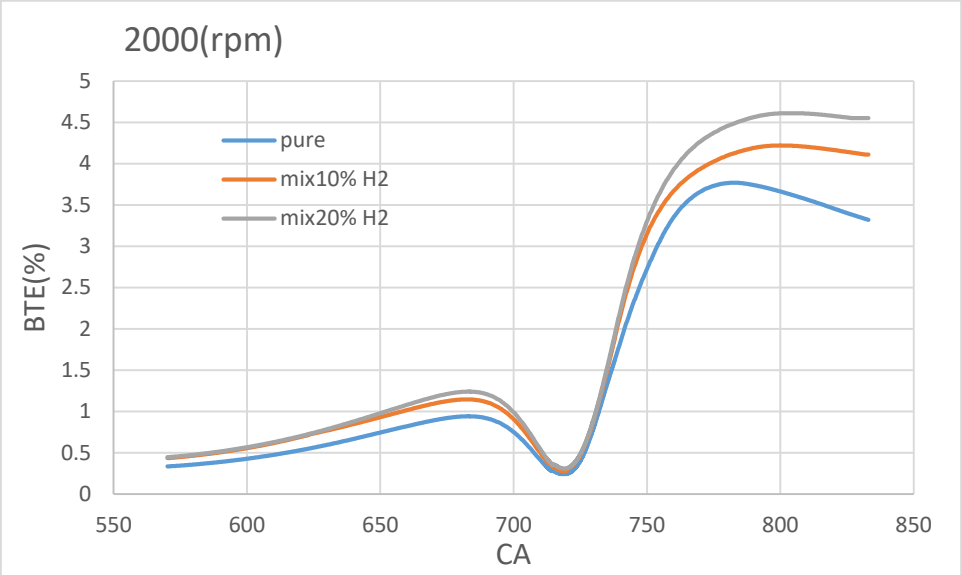

Fig. (7): Break thermal efficiency for pure fuel, 10% and 20% mixing of H_2

3.4. Brake-Specific Fuel Consumption (BSFC)

brake-specific fuel consumption" (BSFC) refers to how much fuel an engine needs to generate a given power output. For varying amounts of H_2 (10% and 20%) mixed with fuel at an engine speed of 2000 rpm, Figure (8) shows the variation in brake-specific fuel consumption. Compared to pure diesel, the brake-specific fuel consumption rates decreased by 10.3% and 19.9%, respectively, when H_2 gas was added to diesel fuel as an accessory fuel at mixing rates of 10% and 20% H_2 gas. The results show that when the amount of H_2 gas delivered to the engine through the air intake manifold increases, the fuel consumption specific to the brakes reduces. H_2 is an oxidizer for fuel, enhancing combustion and boosting combustion efficiency. Comparable outcomes have been achieved in other trials conducted under varying operational conditions [24][25][26].

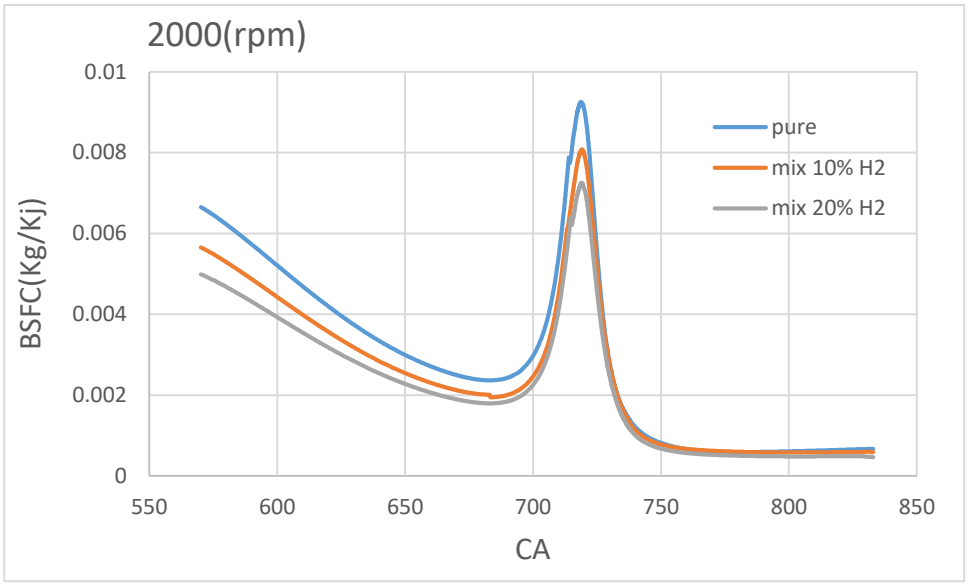

Fig. (8): Brake specific fuel consumption for pure fuel, 10% and 20% mixing of H_2

3.5. Apparent Heat Release Rate (AHRR)

The heat release rate for various H2 percentages (0%, 10%, and 20%) combined with fuel while the engine runs at 2000 rpm is shown in Figure (9). Premixed combustion was shown to be more significantly impacted by hydrogen. Increasing the hydrogen energy integration rate in fuel accelerates the heat release rate. The increased burning velocity and rapid flame propagation speed of hydrogen promotes better combustion and accelerates the rate of combustion, which raises the peak heat release rate significantly.

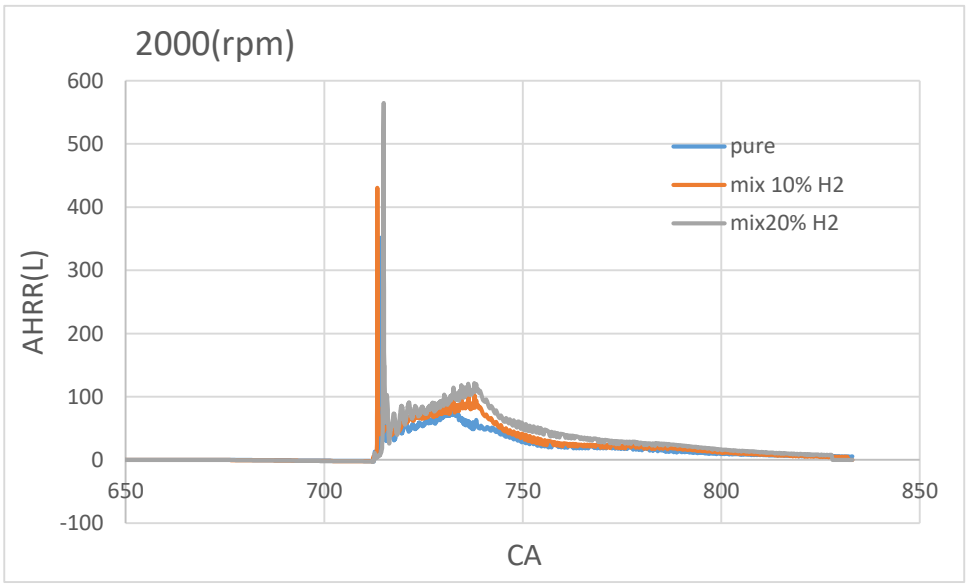

Fig. (9): Apparent heat release rate for pure fuel, 10% and 20% mixing of H_2

3.6. Emission

3.6.1. Carbon Dioxide

Figure (10) shows how the stated CO_2 emissions fluctuate as the H_2 concentration varies. A significant reduction in CO_2 emissions is the outcome of hydrogen enhancement. CO_2 emissions decreased by 25.1% and 39.1%, respectively, with 10% and 20% hydrogen additions. Because hydrogen has no carbon emissions, it produces lower carbon dioxide emissions when combined with diesel fuel [14]. A higher hydrogen-to-carbon (H/C) ratio and a shorter combustion time are achieved when hydrogen is added to diesel fuel; hydrogen has a high flame propagation velocity [12]. Reduced CO_2 emissions result from the improved fuel combustion efficiency, which is caused by the higher hydrogen flame speed, the fuel mixture's superior H/C ratio, and the optimized premixed combustion. Multiple investigations identified similar results in the literature [27] [28].

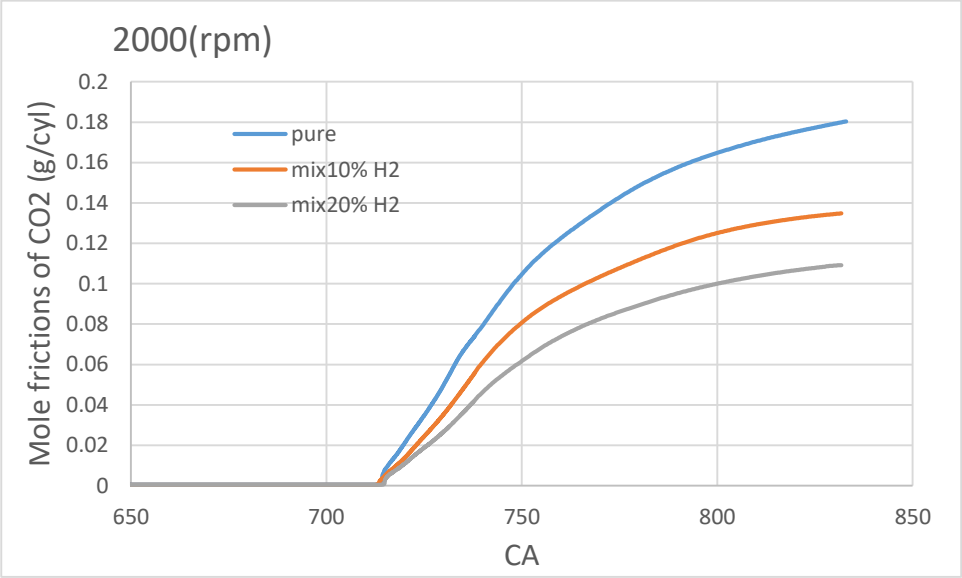

Fig. (10): Mole frictions of CO_2 for pure fuel, 10% and 20% mixing of H_2

Figure (11) depicts the contours of CO_2 production. At 800° CA, the CO_2 generation distributions inside the cylinder can be examined. During the fuel injection (736° CA) and oxidation processes (752° CA), the mole fraction contours of CO_2 continuously decrease as hydrogen intake increases. Significant declines are observed at 800°C.

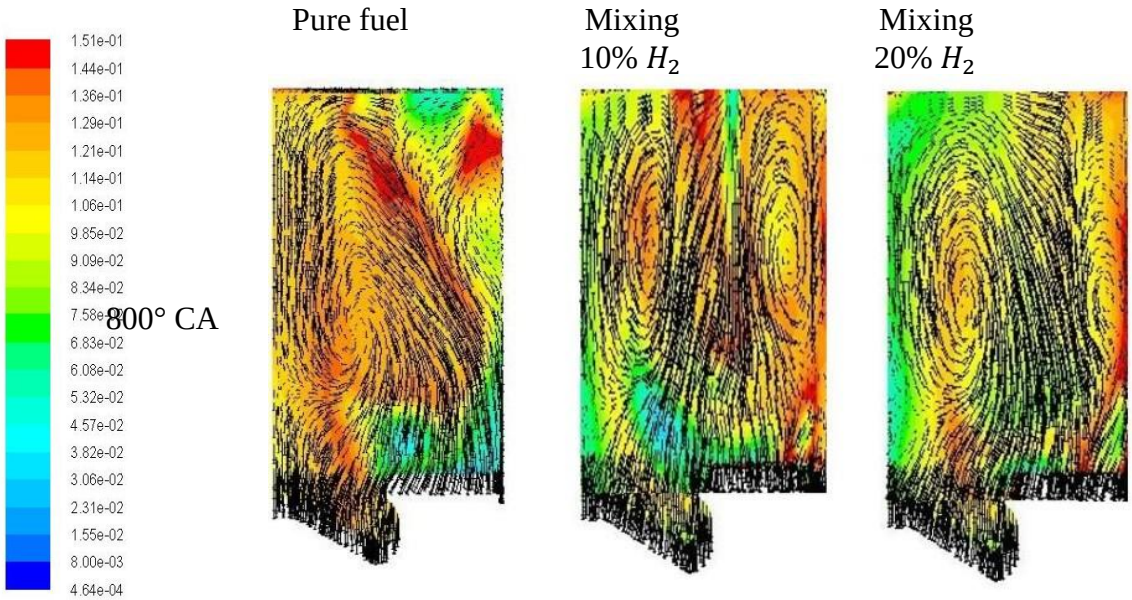

Fig. (11): Mole fraction contours of CO_2 for pure fuel, 10% and 20% mixing of H_2

3.6.2. Carbon Monoxide

The variation in carbon monoxide emissions concerning hydrogen mole fractions is seen in Figure (12). Carbon monoxide (CO) emissions show a consistent trend of decreasing when hydrogen (H_2) is mixed with fuel, down by 57.1% at a 10% volume addition of H_2 and by 64.2% at a 20% volume addition of H_2. Improved combustion efficiency and cylindrical pressure result from the hydrogen's increased flame velocity growth. Also, as hydrogen has a higher diffusivity than other fuels, the combustible mixture is more homogeneous, increasing the amount of oxygen available for optimal combustion [12]. Thus, adding hydrogen reduces CO emissions from lubricating oil and pilot diesel fuel. One may observe the temporal and geographical contours of CO generation within the cylinder for 800° CA, as shown in Figure (13). The findings of this investigation are consistent with the literature [29][30][31].

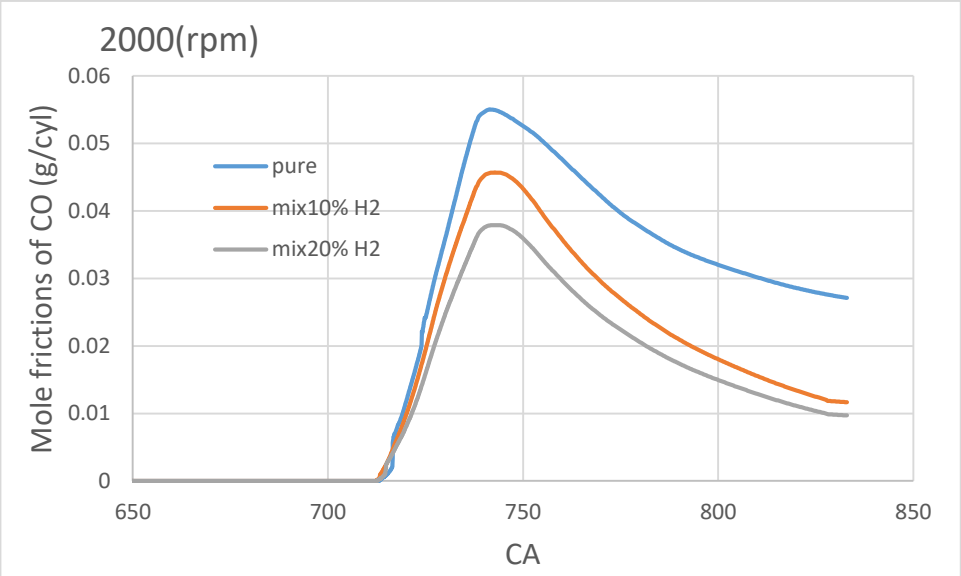

Fig. (12): Mole frictions of CO for pure fuel, 10% and 20% mixing of H_2

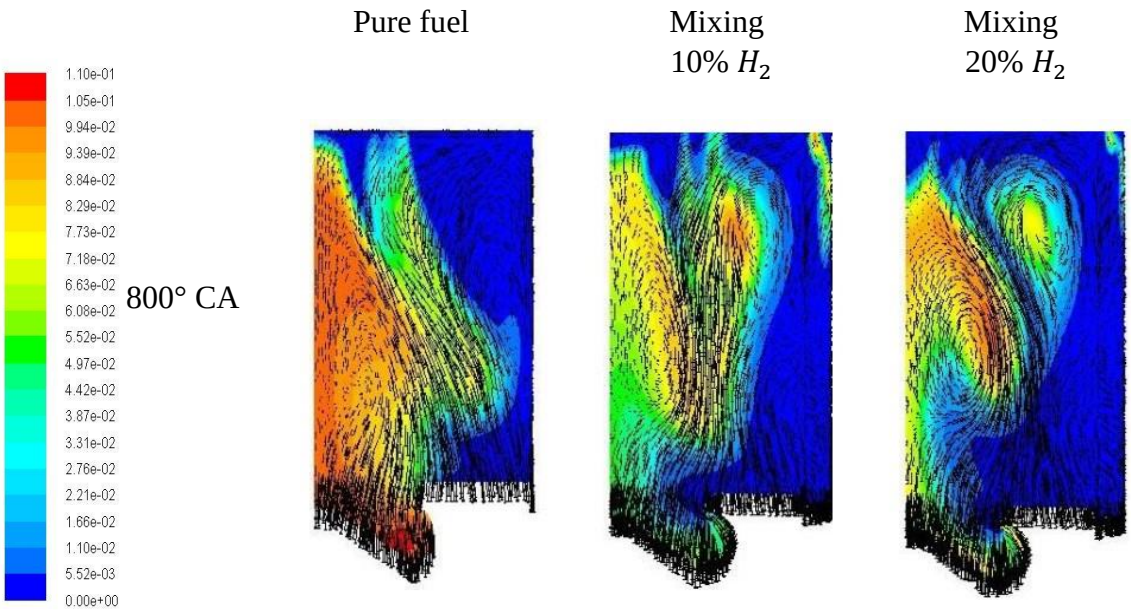

Fig. (13): Mole fraction contours of CO for pure fuel, 10% and 20% mixing of H_2

3.6.3. Nitrogen Oxides Emission

The fluctuations of specific NOx emissions as the H_2 level rises are depicted in Figure (14). It is observed that NOx production has significantly increased. The increase in NOx emission at 10% H_2 and 20% H_2 levels is measured to be 11.4% and 23.2%, respectively, compared to a 0% H_2 content. The reaction time, oxygen percentage, and cylindrical temperature are all related to NOx production [16]. Because hydrogen burns faster than diesel, there is a greater chance that diesel

will burn completely when added to the combustion process. The in-cylinder temperature rises due to complete combustion, raising the peak pressure [21]. The higher peak in-cylinder temperatures caused by hydrogen's lower heating value (LHV) than diesel fuel are also responsible for the rise in NOx emissions [16]. Similar results were obtained in the experimental examinations of the literature [29][31][32]. Figure (15) depicts the curves of NOx production. The distributions of NOx generation within the cylinder can be examined at 800° CA.

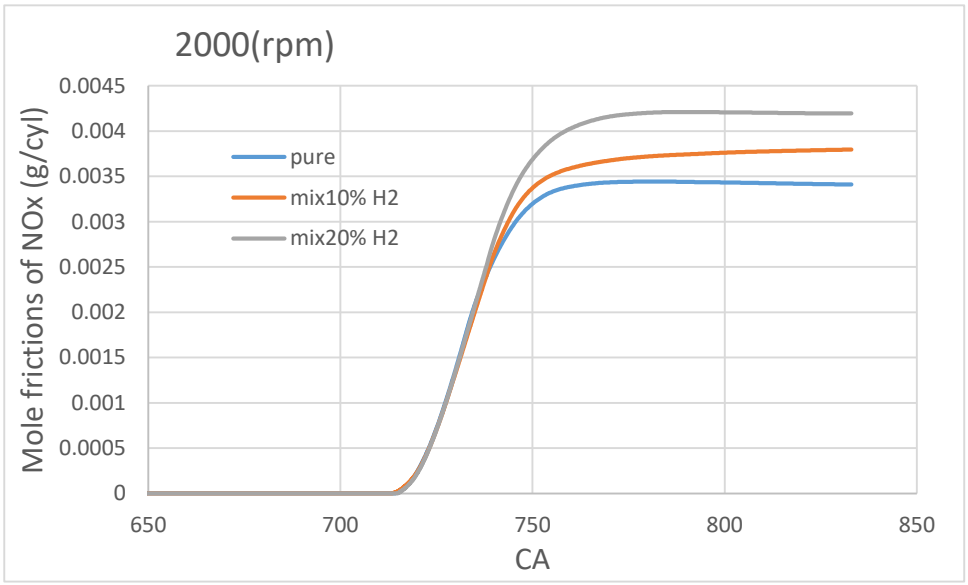

Fig. (14): Mole frictions of NOx for pure fuel, 10% and 20% mixing of H_2

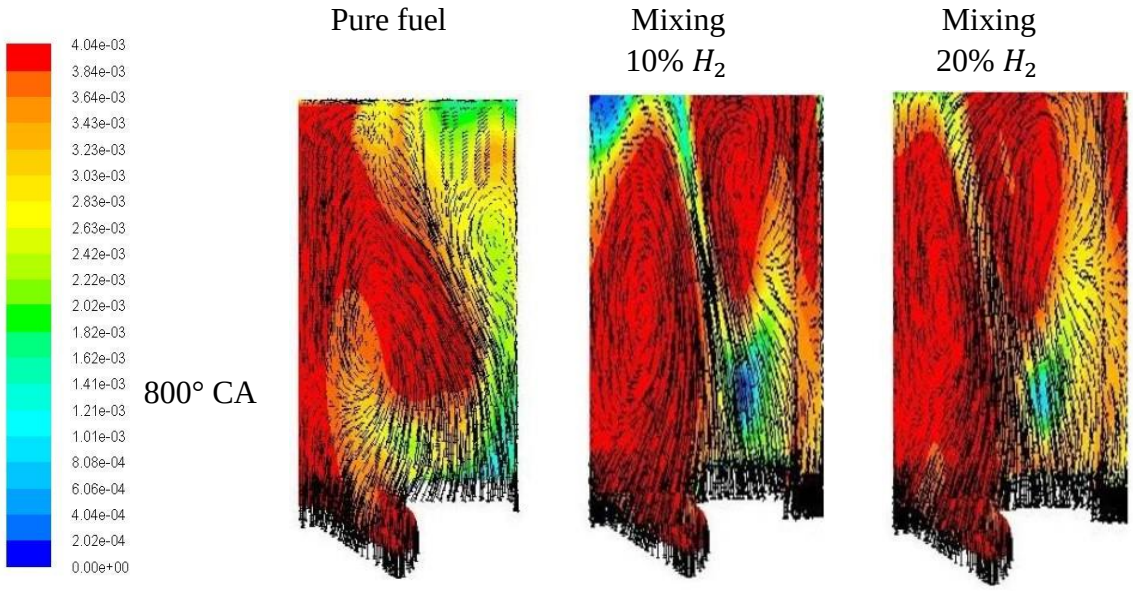

Fig. (15): Mole fraction contours of NO_x for pure fuel, 10% and 20% mixing of H_2

4. Conclusions

This paper aimed to analyze the performance, combustion properties, and emission characteristics of n-heptane combustion in internal combustion engines (IC engines) with hydrogen assistance. In order to achieve this, three-dimensional numerical simulations were run on an engine powered by n-heptane and mixed with hydrogen at 10% and 20% by volume. The modeling data can be used to evaluate the homogeneity of the hydrogen-fuel mixture's structure to improve engine performance and combustion.

The following conclusions can be derived:

1. Introducing hydrogen into the engine elevates cylinder pressure due to improved combustion, resulting in pressure increases of 4.1% and 15.9% for 10% and 20% of hydrogen levels, respectively.
2. All investigations demonstrated a substantial enhancement in brake thermal efficiency, with the most notable gains being 23.7% and 37% for 10% and 20% of hydrogen levels, respectively.
3. Brake specific fuel consumption decreased, with the most significant reductions being 10.3% and 19.9% when 10% and 20% using hydrogen with fuel compared to pure fuel. The findings suggest that the dual-fuel technique is more economically advantageous.
4. Carbon emissions diminished with the augmentation of hydrogen induction into the engine, resulting in reductions of 57.1% and 64.2% for carbon monoxide. Furthermore, the decreases in carbon dioxide are 25.1% and 39.1% for 10% and 20% of hydrogen levels, respectively.
5. A downside of utilizing hydrogen as fuel in internal combustion engines is its role in elevating nitrogen oxide emissions, with increases of 11.4%, and 23.2% for 10% and 20% of hydrogen levels, respectively.

Acknowledgment

The author expresses gratitude to the University of Thi-Qar and the supervising professor, Dr. Rafid Mallak Hannun, for their assistance and guidance while preparing this research.

Nomenclatures

Symbol	Description
AHRR	Apparent heat release rate
BSFC	Brake-specific fuel consumption
BTE	Brake thermal efficiency
CA	Crank angel
CFD	Computational Fluid Dynamics
CO	Carbon monoxide
CO_2	Carbon dioxide
EGR	Exhaust Gas Recirculation
EU	European Union
EVO	Indicated mean effective pressure
FCEV	Fuel cell electric vehicles
GHG	Greenhouse gas
H_2	Hydrogen
H_2ICE	Hydrogen-fueled internal combustion engines
HC	Hydrocarbon
ICE	Internal combustion engines
IMEP	Exhaust valve opened
IVC	Energy availability
LHV	Lower heating value
NOx	Nitrogen Oxides
RPM	Revolution per minutes
SL	Flame speed
TDC	Top dead center

Author Contributions Statement: Both authors contributed to the Conception; Methodology; Experiments; Data Analysis and Interpretation; Writing – Original Draft; Writing – Review & Editing. Both authors have read and approved the final version of the manuscript.

References

[1] K. R. Patil, P. M. Khanwalkar, S. S. Thipse, K. P. Kavathekar, and S. D. Rairikar, "Development of HCNG blended fuel engine with control of NOx emissions," in *2009 Second International Conference on Emerging Trends in Engineering & Technology*, IEEE, 2009, pp. 1068–1074. https://doi.org/10.1109/ICETET.2009.81

[2] C. Fetting, "The European green deal", *ESDN Report, December*, vol. 2, no. 9, p. 53, 2020.

[3] M. Zahid and K. S. Syed, "Investigation of pollutants formation in a diesel engine using numerical simulation", *Advanced Modeling and Simulation in Engineering Sciences*, vol. 8, no. 1, 2021. https://doi.org/10.1186/s40323-021-00204-6.

[4] Z. Stępień, "A comprehensive overview of hydrogen-fueled internal combustion engines: Achievements and future challenges", *Energies*, vol. 14, no. 20, p. 6504, 2021. https://doi.org/10.3390/en14206504.

[5] L. Estrada, E. Moreno, A. Gonzalez-Quiroga, A. Bula, and J. Duarte-Forero, "Experimental assessment of performance and emissions for hydrogen-diesel dual fuel operation in a low displacement compression ignition engine", *Heliyon*, vol. 8, no. 4, p. e09285, 2022. https://doi.org/10.1016/j.heliyon.2022.e09285.

[6] R. Kavtaradze, T. Natriashvili, and S. Gladyshev, "Hydrogen-diesel engine: Problems and prospects of improving the working process", *SAE Technical Paper*, 2019. https://doi.org/10.4271/2019-01-0541.

[7] H. Koten, "Hydrogen effects on the diesel engine performance and emissions", *International journal of hydrogen energy*, vol. 43, no. 22, pp. 10511–10519, 2018. https://doi.org/10.1016/j.ijhydene.2018.04.146.

[8] X. Zhang, J. Hu, B. Wang, Z. Li, S. Xu, and X. Ma, "A chiral zinc(II) metal-organic framework as a high selective luminescent sensor for detecting trace nitro explosives picric acid and Fe3+ ion", *Journal of Solid State Chemistry*, vol. 269, pp. 459–464, 2019, doi https://doi.org/10.1016/j.jssc.2018.10.021.

[9] A. Demirci, H. Koten, and M. Gumus, "The effects of small amount of hydrogen addition on performance and emissions of a direct injection compression ignition engine", *Thermal science*, vol. 22, no. 3, pp. 1395–1404, 2018. https://doi.org/10.2298/TSCI170802004D.

[10] M. Sughayyer, "Effects of hydrogen addition on power and emissions outputs from diesel engines", *Journal of Power and Energy Engineering*, vol. 4, pp. 47-65, 2016. http://dx.doi.org/10.4236/jpee.2016.41003.

[11] M. Loganathan, A. Velmurugan, T. Page, E. J. Gunasekaran, and P. Tamilarasan, "Combustion analysis of a hydrogen-diesel fuel operated DI diesel engine with exhaust gas recirculation", *Frontiers in Energy*, vol. 11, pp. 568–574, 2017. https://doi.org/10.1007/s11708-017-0461-y.

[12] O. H. Ghazal, "Performance and combustion characteristic of CI engine fueled with hydrogen enriched diesel", *International journal of hydrogen energy*, vol. 38, no. 35, pp. 15469–15476, 2013. https://doi.org/10.1016/j.ijhydene.2013.09.037.

[13] M. Deb, G. R. K. Sastry, P. K. Bose, and R. Banerjee, "An experimental study on combustion, performance and emission analysis of a single cylinder, 4-stroke DI-diesel engine using hydrogen in dual fuel mode of operation", *International journal of hydrogen energy*, vol. 40, no. 27, pp. 8586–8598, 2015. https://doi.org/10.1016/j.ijhydene.2015.04.125.

[14] Y. Karagöz, T. Sandalcı, L. Yüksek, A. S. Dalkılıç, and S. Wongwises, "Effect of hydrogen–diesel dual-fuel usage on performance, emissions and diesel combustion in diesel engines", *Advances in Mechanical Engineering*, vol. 8, no. 8, p. 1687814016664458, 2016. https://doi.org/10.1177/1687814016664458.

[15] A. M. De Morais, M. A. M. Justino, O. S. Valente, S. de Morais Hanriot, and J. R. Sodré, "Hydrogen impacts on performance and CO2 emissions from a diesel power generator", *International Journal of Hydrogen Energy*, vol. 38, no. 16, pp. 6857–6864, 2013. https://doi.org/10.1016/j.ijhydene.2013.03.119.

[16] H. Köse and M. Ciniviz, "An experimental investigation of effect on diesel engine performance and exhaust emissions of addition at dual fuel mode of hydrogen", *Fuel processing technology*, vol. 114, pp. 26–34, 2013. https://doi.org/10.1016/j.fuproc.2013.03.023.

[17] R. Adnan, H. H. Masjuki, and T. M. I. Mahlia, "Experimental investigation on in-cylinder pressure and emissions of diesel engine with port injection hydrogen system", *International Journal of Mechanical and Materials Engineering*, vol. 5, no. 2, pp. 136–141, 2010.

[18] F. S. D. Almutairi, "Modelling and simulation of combustion characteristics of hydrogen-enriched

dual-fuel combustion", *University of Southampton, Doctoral Thesis*, pp. 283, 2022. https://doi.org/10.1016/j.ijhydene.2022.10.078.

[19] H. K. Versteeg, "An introduction to computational fluid dynamics the finite volume method", *2/E. Pearson Education India*, 2007.

[20] M. C. R. Martins, "3D CFD Combustion Simulation of a Four-Stroke SI Opposed Piston IC Engine", *Universidade da Beira Interior (Portugal) ProQuest Dissertations & Theses*, 2020.

[21] H. An, W. M. Yang, A. Maghbouli, J. Li, S. K. Chou, K. J. Chua, J. X. Wang, and L. Li, "Numerical investigation on the combustion and emission characteristics of a hydrogen assisted biodiesel combustion in a diesel engine", *Fuel*, vol. 120, pp. 186–194, 2014. https://doi.org/10.1016/j.fuel.2013.12.021.

[22] Y. Song, L. Marrodán, N. Vin, O. Herbinet, E. Assaf, C. Fittschen, A. Stagni, T. Faravelli, M.U. Alzueta, and F. Battin-Leclerc, "The sensitizing effects of NO2 and NO on methane low temperature oxidation in a jet stirred reactor", *Proceedings of the Combustion Institute*, vol. 37, no. 1, pp. 667–675, 2019. https://doi.org/10.1016/j.proci.2018.06.115.

[23] S. Bari and M. Mohammad Esmaeil, "Effect of H2/O2 addition in increasing the thermal efficiency of a diesel engine," *Fuel*, vol. 89, no. 2, pp. 378–383, 2010. https://doi.org/10.1016/j.fuel.2009.08.030.

[24] X. Liu, S. Liu, L. Shen, Y. Bi, and L. Duan, "Study on the Effects of the Hydrogen Substitution Rate on the Performance of a Hydrogen–Diesel Dual-Fuel Engine under Different Loads", *Energies*, vol. 16, no. 16, 2023. https://doi.org/10.3390/en16165971.

[25] J. Luo, Z. Liu, J. Wang, H. Xu, Y. Tie, D. Yang, and Z. Zhang, "Effects of Hydrogen Addition on the Performance, Combustion, and Emission Characteristics of a Heavy-Duty Dual-Fuel Engine", *SSRN*, pp. 49, 2022. https://dx.doi.org/10.2139/ssrn.4110723.

[26] N. Abbas, M. A. Badshah, M. B. Awan, and N. Zahra, "Performance and Gaseous Emission Investigation of Low Powered Spark Ignition Engine Fueled with Gasoline and Hydroxyl Gas: Hydroxyl Gas-gasoline Mixture Engine", *Proceedings of the Pakistan Academy of Sciences: A. Physical and Computational Sciences*, vol. 55, no. 1, pp. 11–20, 2018.

[27] W. Tutak, A. Jamrozik, and K. Grab-Rogaliński, "Co-Combustion of Hydrogen with Diesel and Biodiesel (RME) in a Dual-Fuel Compression-Ignition Engine", *Energies*, vol. 16, no. 13, p. 4892, 2023. https://doi.org/10.3390/en16134892.

[28] B. Swapnil, and S. C. Omkar, "Study of Performance and Emission Analysis of Hydrogen-Diesel Dual Fuel Engine", no. May, pp. 1214–1218, 2019.

[29] P. Karvounis and G. Theotokatos, "Diesel Substitution with Hydrogen for Marine Engines", *Proceedings of the 4th International Conference on Modelling and Optimisation of Ship Energy Systems, 2023*, TU Delft OPEN Publishing, 2024. https://doi.org/10.59490/moses.2023.657.

[30] A. Shaafi, M. J. Noroozi, and V. Manshaei, "Investigating the effects of fuel injection strategies on a dual-fuel diesel-h2 compression ignition engine", *Journal of Computational & Applied Research in Mechanical Engineering*, vol. 10, no. 1, pp. 63–71, 2020. https://doi.org/10.22061/jcarme.2019.5430.1675.

[31] J. T. Mcnally, and C. R. Koch, "Hydrogen-Diesel Dual Fuel Combustion Characterization", *Diss. Ph. D. thesis), University of Alberta*, 2023.

[32] L. Xu, H. Dong, S. Liu, L. Shen, and Y. Bi, "Study on the Combustion Mechanism of Diesel/Hydrogen Dual Fuel and the Influence of Pilot Injection and Main Injection", *Processes*, vol. 11, no. 7, p. 2122, 2023. https://doi.org/10.3390/pr11072122.